

Received March 21, 2021, accepted March 27, 2021, date of publication April 5, 2021, date of current version May 3, 2021.

Digital Object Identifier 10.1109/ACCESS.2021.3071121

Optimal Scheduling of Cooling and Power Combined Supply System for Tropical Renewable Microgrids

JUNYU LIANG¹, ZHAO LUO¹ ², (Member, IEEE), XINGYU YUAN¹, JIALU GENG², HONGZHI LIU², JIAQUAN YANG¹, MIN DONG², AND YINGHAO DAI²

¹Electric Power Institute, Yunnan Power Grid Company Ltd., Kunming 650217, China

²Faculty of Electric Power Engineering, Kunming University of Science and Technology, Kunming 650500, China

Corresponding author: Zhao Luo (waiting.1986@live.com)

This work was supported in part by the National Natural Science Foundation of China under Grant 51907084, in part by the Science and Technology Project of Yunnan Power Grid Company Ltd., under Grant YNKJXM20190087, in part by the Applied Basic Research Foundation of Yunnan Province under Grant KKS0202104007, and in part by the Scientific Research Foundation of the Yunnan Provincial Department of Education under Grant 2018JS032.


ABSTRACT To satisfy the residential cooling demand in tropical large renewable microgrids (MGs), multiple ice-storage air conditionings (IACs) are usually used to supply cold energy. However, these IACs could not directly exchange the cold energy, which seriously limits the combined regulation effect. To address the problem, a novel cooling and power combined supply system (CPCSS) is proposed in this paper, where the trucks are used to distribute the ices among IACs. To evaluate the performance on the multi-time scales, a cooling and power combined supply model is established. On this basis, a two-stage (i.e., day-ahead and real-time stage) scheduling strategy is presented to minimize the MG operation cost. To speed up the solution, this scheduling model is first linearized as a classic mixed-integer second-order cone programming (MISCP) problem, and then is solved by Lagrange solution method. Simulation studies on an IEEE 14-node system indicates that compared with the existing MG operation cost, the annual operational cost of the based-two-truck CPCSS could be reduced by 9868800 yuan (12.6%), while the network loss could be decreased from 5.4 to 3.9 MWh. The results confirm the effectiveness of the proposed strategy.

INDEX TERMS Renewable microgrid, ice-storage air conditioning, multi-time scale, cooling and power combined supply system, Lagrange solution.

I. INTRODUCTION

Energy crisis and environmental awareness stimulate the large-scale renewable energy connected to grid [1], [2]. However, the randomness and volatility of renewable generation also bring great challenges to the safe and economic operation of power grid [3], [4]. Research shows that multi-energy systems could mitigate the bad impact of the renewable generation while developing complementary advantage [5]. Benefiting from this, integrated heat, cooling, and power systems are believed to be more and more popular in the future. Therefore, it is of great practical significance to study the optimal scheduling of the integrated heat, cooling and power system.

Actually, the heat, (cooling,) and power combined scheduling has been an active research field for a long time. For

The associate editor coordinating the review of this manuscript and approving it for publication was Ali Raza .

example, a heat current model of a district heating network is constructed in [6] to deduce the corresponding heat transport matrix by applying Ohm's and Kirchhoff's laws. A flexibility evaluation method based on a generalized thermal storage model is introduced in [7] to systematically characterize and quantify the flexibility of district heating networks in combined heat and power dispatch. A uniform framework in the Laplace domain is formulated in [8] by modeling heat losses and transfer delays from an electrical-analog perspective. The transient heat flow and steady-state electric power flow are combined in [9] to formulate the dynamic optimal energy flow model of the heat and electricity integrated energy system. On this basis, an end-to-end district heating system model is developed in [10] to consider pipeline energy storage with an explicit relationship between heat generation and demand. A combined heat and power dispatch model is formulated in [11] to coordinate the operation of electric power system and district heating system considering

pipeline energy storage. Transmission constrained unit commitment with combined electricity and district heating networks is used in [8], [12] to accommodate large amounts of variable wind power by utilizing the heat storage capacity of district heating systems. A decentralized operation scheme for interdependent power distribution network and district heating network is designed in [13] to create additional opportunities of spatial and temporal demand response. A decentralized and parallel dispatching method for the operation of the integrated heat and electricity systems is used in [14] to coordinate a high resolution of electricity and heat dynamics. A two-level supervisory closed-loop feedback strategy is discussed in [3], where the lower level processes only local measurements, and the upper level updates the local controllers to minimize thermal discomfort of the microgrid. A two-stage robust integrated electricity and heating system scheduling model is proposed in [15] to deal with the uncertainties of the heat load, ambient temperature and heat dissipation coefficients of heating pipelines. A new stochastic model based on the energy hub approach is developed in [16] to treat the external dependencies and their uncertainty referring to heat and power systems. The above work almost focuses on the thermal energy supply based on district heating networks. However, in the tropical regions, the residential cooling demand is the main consideration. Unlike the heat which could be transmitted over a long distance, the cold energy usually flows locally due to the serious energy leakage. Therefore, we may not directly learn a lot from the above modelling method or optimization strategy.

More recently, more and more researchers have focused on the cooling and power combined scheduling. For example, residential refrigeration technologies are presented in [17] to coordinate the power generation and energy storage. A comprehensive analysis of an office building performances is outlined in [18] to analyze the refrigeration energy consumption and thermal comfort. A novel cooling system based on phase change materials is proposed in [19], [20] to satisfy the residential cooling demands. The use of variable speed drives is discussed in [21] for cost-effective energy savings in South African mine cooling systems. A novel implementation strategy is formulated in [22] for mine cooling systems to improve the energy utilization. A newly developed open source data center package in the Modelica Buildings library is introduced in [23] to support modeling and simulation of cooling and control systems of data centers. Physics based models are developed in [24] to allow the prediction of the energy consumption and heat transfer phenomenon in a data center. A supervisory control strategy is studied in [25] for an indirect adiabatic cooling system with application to data centers. The optimization problem of data center cooling system is formulated as an integer linear programming problem and solved using a heuristic algorithm in [26]. A new mathematical model is proposed in [27] to map the effect of ambient temperature to the aggregate demand response of a heterogeneous population of air conditionings. A coordinated

control strategy is designed in [28] for inverter and fixed air conditioning to cool the residents while carrying out the frequency regulation. An optimal control method for ice-storage air conditioning (IAC) based on reducing sequentially direct cooling cost is proposed in [29]. An optimal dispatch model of an IAC system for participants is established in [30] to quickly and accurately perform energy saving and demand response. Particle swarm algorithm is adopted in [31] to facilitate optimization of IAC systems and to develop optimal operating strategies, using minimal life cycle cost as the objective function. However, the above cooling systems could not transmit the cold energy over a long distance and exchange energy between each other, which seriously limits cooling and power combined scheduling benefits. Additionally, focusing on the power consumption shifting characteristic on the long-time scale, the above literature rarely notices the regulation flexibility of cooling systems on the short-time scale. Finally, the existing works usually study the cooling and power combined performance using the DC power flow model, which may result in a large error due to the ignorance of the network loss.

With the above observation, it is speculated that more energy exchange between cooling and power system could better develop the complementary advantages and coordination benefits. Therefore, this paper attempts to make some improvements on the IAC scheduling. First, inspired by the ice delivering for resident heat dissipation and supermarket meat preservation [32], a novel cooling and power combined system (CPCSS) for tropical microgrids (MGs) is proposed, where trucks are used to transport and distribute the ice among IACs. Considering the consumption shifting and power smoothing ability of the IACs, a cooling and power combined supply model on the multi-time scales is established. Additionally, to ensure the cooling and power combined supply performance, a two-stage (i.e., day-ahead stage and real-time stage) MG scheduling strategy is formulated. On this basis, linear techniques are first used to convert this MG scheduling model into a classic mixed-integer second-order cone programming problem (MISCP), followed by Lagrange solution method. The simulation studies are conducted on IEEE 14-node distribution network. The main contributions are presented as follows:

- 1) A novel integrated cooling and power system for tropical MGs is proposed. Benefiting from this, the complementary advantages of integrated cooling and power system are further developed.

- 2) A novel cooling and power combined supply model on multi-time scales is established. On this basis, a two-stage scheduling strategy is designed to carry out consumption shifting and power smoothing simultaneously.

- 3) The MG scheduling model is first linearized and efficiently solved by Lagrange solution method. Additionally, the effectiveness and benefits of the proposed model is verified using realistic renewable generation and load.

II. COOLING AND POWER COMBINED SUPPLY MODE FOR ISLANDED MICROGRIDS

A. OPERATIONAL MECHANISM OF THE ICE-STORAGE AIR CONDITIONERS

Figure. 1 shows the operational mechanism of ice-storage air conditionings (IACs). As observed from the figure, IACs consist of the ice maker, ice melting unit, and refrigeration unit. The ice maker can produce ices and store them into ice storage banks. By consuming these storage ices, the ice melting unit could supply cold energy. Additionally, the cooling demands are also able to be satisfied using refrigeration unit. It can be seen that the IACs have a certain flexible regulation ability. Therefore, the IACs could be used to respond to the grid demand while supplying the local cooling load.

However, the cooling flow cannot be transmitted over a long distance due to serious energy loss. In this case, multiple IACs need to be installed. Because the cooling energy could not be exchanged directly, the energy saving performance may not be good enough even if multiple IACs are operated jointly.

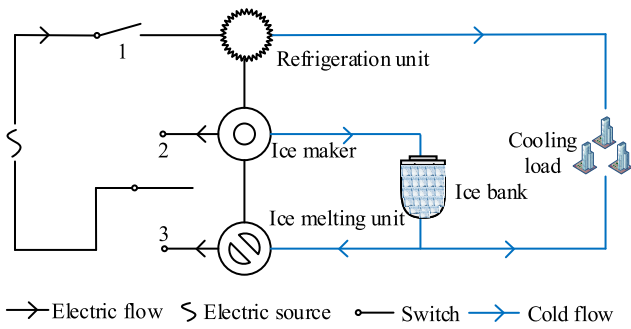


FIGURE 1. Diagram of ice-storage air conditioner.

B. COOLING AND POWER COMBINED SUPPLY SYSTEM

Figure. 2 depicts a novel CPCSS. As observed from the figure, multiple IACs are connected to MGs to satisfy the cooling demand. The ices are produced and stored in the tanks of the IACs. To achieve the cold energy exchange, trucks are used to carry, transfer, and distribute the storage ices among the IACs. By this means, the electric transmission loss may be reduced significantly. Therefore, the cooling and power energy could be better supplied. Note that the CPCSS could be regulated flexibly on the multiple time scales, which is introduced in details in section III.

III. OPERATIONAL MODEL OF THE COOLING-POWER COMBINED SUPPLY SYSTEM ON MULTI-TIME SCALE

In this section, the CPCSS operational model on the multi-time scales is established.

A. CPCSS MODEL ON THE COOLING SIDE

Multiple IACs with trucks are combined to satisfy the cooling demands. They are operated with the time-space network constraints and time-energy limits. The time-space network constraints are presented in (1)-(6), where (1) expresses the

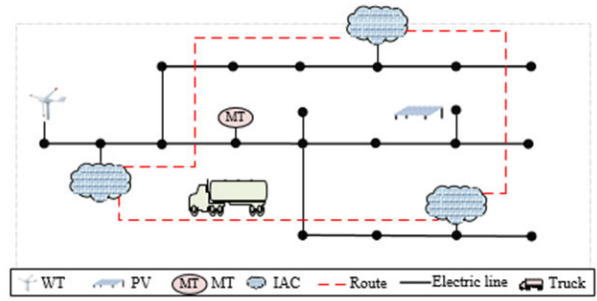


FIGURE 2. Structure of the CPCSS applied to islanded MGs.

truck k has only one position at time t , (2) denotes that the truck space position should be connected with each other, (3)-(4) limit the truck travel time from station i to j , (5) stands for the constraint of the truck initial position, (6) requires that the truck k returns to its original position at the end.

$$\sum_{ij} Z_t^{k,ij} = 1 \tag{1}$$

$$Z_{t+1}^{k,ij} + Z_{t+1}^{k,ji} \geq Z_t^{k,ij} \tag{2}$$

$$Z_{t+T^{ij}+1}^{k,ij} \geq Z_t^{k,ii} \quad \forall t = 1, \dots, T - T^{ij} - 1 \tag{3}$$

$$\sum_{\tau=t}^{t+T^{ij}-1} Z_{\tau}^{k,ij} \geq (Z_t^{k,ij} - Z_{t-1}^{k,ij}) T^{ij} \tag{4}$$

$$\sum_i Z_1^{k,ij} \geq Z_0^{k,ij} \tag{5}$$

$$Z_T^{k,ii} = Z_0^{k,ii} \tag{6}$$

where the binary variable $Z_t^{k,ij} = 1$ represents the truck k is driving from station i to j at time t , vice versa, T^{ij} expresses the driving time from station i to j , and T is the scheduling cycle.

The time-energy constraints of the trucks are given in (7)-(14), where (7) means the ice throughput constraint of truck k , (8) expresses that the truck ice load at time t is determined by ice load at time $t-1$ and ice throughput at time t , (9)-(10) are the truck loading ice limits, (11) represents that the IAC ice storage capacity is related with the ice making power, ice melting power, and ice throughput, (12)-(13) indicate the ice storage constraints of the IACs, and (14) stands for the balance between the cold supply and cooling demand [29].

$$|H_t^{ice,k,i}| \leq H_m^{ice,k} Z_t^{k,ii} \tag{7}$$

$$E_t^{ice,k} = E_{t-1}^{ice,k} \xi^{air} + \sum_i H_t^{ice,k,i} \tag{8}$$

$$0 \leq E_t^{ice,k} \leq E_m^{ice} \tag{9}$$

$$E_T^{ice,k} = E_0^{ice,k} \tag{10}$$

$$E_t^{AC,i} = E_{t-1}^{AC,i} \xi^{air} + P_t^{icemaking,i} \eta^{icemaking} - P_t^{melt,i} \eta^{melt} - \sum_k H_t^{ice,k,t} \tag{11}$$

$$0 \leq E_t^{AC,i} \leq E_m^{AC,i} \tag{12}$$

$$E_T^{AC,i} = E_0^{AC,i} \quad (13)$$

$$P_t^{chiller,i} \eta^{chiller} + P_t^{melt,i} \eta^{melt} = H_t^{l,i} \quad (14)$$

where $H_t^{ice,k,i}$ and $H_m^{ice,k}$ are the actual and rated ice throughput amount, respectively, ξ^{air} is the ice retention rate considering the cold leakage, $E_t^{ice,k}$ and E_m^{ice} are the actual and rated ice storage amount of the truck, respectively, $P_t^{icemaking,i}$, $P_t^{melt,i}$, and $P_t^{chiller,i}$ are the ice making power, ice melting power, and refrigeration power, respectively, $\eta^{icemaking}$, η^{melt} , and $\eta^{chiller}$ are the ice making efficiency, ice melting efficiency, and refrigeration efficiency, respectively, $E_{t-1}^{AC,i}$ and $E_m^{AC,i}$ are the actual and rated ice storage amount of the IACs, respectively, and $H_t^{l,i}$ is the cooling demand at time t .

B. CPCSS MODEL ON THE ELECTRIC SIDE

On the electric side, the IAC working power constraints and power flow limit shall be considered. The refrigeration power, ice making power, and melting power of IACs shall be constrained to following formulas:

$$0 \leq P_t^{chiller,i} \leq P_m^{chiller,i} \quad (15)$$

$$0 \leq P_t^{icemaking,i} \leq P_m^{icemaking,i} \quad (16)$$

$$0 \leq P_t^{melt,i} \leq P_m^{melt,i} \quad (17)$$

where $P_m^{chiller,i}$, $P_m^{icemaking,i}$, and $P_m^{melt,i}$ are the rated power of refrigeration, ice making, and ice melting, respectively.

Additionally, the power flow constraints are given in (18)-(26), where (18)-(19) express the active and reactive injection power constraints of nodal i , respectively, (20)-(21) represent the relationship between the node injection power and branch power, (22)-(23) are the active and reactive power limits at the head and end of the branch ij , respectively, (24)-(26) stand for the nodal voltage and branch line constraints [33].

$$P_t^i = P_t^{l,t} + P_t^{icemaking,i} + P_t^{melt,i} + P_t^{chiller,i} - P_t^{WT,i} - P_t^{PV,i} - P_t^{g,i} \quad (18)$$

$$Q_t^i = Q_t^{l,t} + Q_t^{icemaking,i} + Q_t^{melt,i} + Q_t^{chiller,i} - Q_t^{WT,i} - Q_t^{PV,i} - Q_t^{g,i} \quad (19)$$

$$P_t^i = - \sum_j \frac{P_t^{ij}}{j} \quad (20)$$

$$Q_t^i = - \sum_j \frac{Q_t^{ij}}{j} \quad (21)$$

$$P_t^{ij} = P_t^i - r^{ij} \ell_t^{ij} \quad (22)$$

$$Q_t^{ij} = Q_t^i - x^{ij} \ell_t^{ij} \quad (23)$$

$$\ell_t^{ij} = \left((P_t^{ij})^2 + (Q_t^{ij})^2 \right) / v_t^i \quad (24)$$

$$\ell_t^{ij} \leq \bar{\ell}^{ij} \quad (25)$$

$$v_t^j \leq v_t^i \leq \bar{v}^i \quad (26)$$

where P_t^i is the nodal injection active power, $P_t^{l,t}$ is the load active power, $P_t^{WT,i}$, $P_t^{PV,i}$, and $P_t^{g,i}$ are the active power of the

wind turbine (WT) generation, photovoltaic (PV) output, and micro turbine (MT) generation, respectively, Q_t^i , $Q_t^{l,t}$, $Q_t^{WT,i}$, $Q_t^{PV,i}$, and $Q_t^{g,i}$ are the corresponding reactive power, P_t^{ij} and Q_t^{ij} are the active and reactive power at the head of the branch ij , respectively, ℓ_t^{ij} is the current square of branch ij , r^{ij} and x^{ij} stand for the branch resistance and reactance, respectively, $\bar{\ell}^{ij}$ is the rated current square of branch ij , v_t^i , \underline{v}^i , and \bar{v}^i mean the real-time, minimum, and maximum voltage square of node i , respectively.

The CPCSS operational model would be scheduled using a two-stage scheduling strategy, which is explained in Section IV.

IV. TWO-STAGE SCHEDULING STRATEGY

To ensure the cooling and power combined supply performance on multi-time scales, a two-stage scheduling strategy is proposed, where the day-ahead stage optimizes ice transportation routes, and the real-time stage determines the optimal unit operation power.

A. DAY-AHEAD SCHEDULING STAGE

In the day-ahead stage, renewable generation forecasting errors may impact the microgrid operation costs consisting of the MT generation cost and truck fuel cost. To mitigate the impact, stochastic optimization method is used in this paper to determine a reasonable day-ahead decision. The details are presented as follows:

First, according to the existing forecasting technology or consulting relevant departments, Photovoltaic generation $P_t^{PV,i}$, wind output $P_t^{WT,i}$, and forecasting error could be easily obtained. Without loss of generality, assume that the distribution laws of forecasting errors satisfy (27)-(28) [34]. On this basis, Monte Carlo sampling method is used to generate lots of possible power scenarios. Finally, to reduce the computation burden, scenario reduction method is used to obtain limited typical scenarios, where the wind generation and PV output in node i in scenario s are denoted as $P_t^{PV,i}$ and $P_t^{WT,i}$.

$$f(P_t^{PV}) = \frac{1}{P_m^{PV} B(\alpha_1, \beta_1)} \left(\frac{P_t^{PV}}{P_m^{PV}} \right)^{\alpha_1-1} \left(1 - \frac{P_t^{PV}}{P_m^{PV}} \right)^{\beta_1-1} \quad (27)$$

$$f(P_t^{Wind}) = \frac{1}{P_m^{Wind} B(\alpha_2, \beta_2)} \left(\frac{P_t^{Wind}}{P_m^{Wind}} \right)^{\alpha_2-1} \left(1 - \frac{P_t^{Wind}}{P_m^{Wind}} \right)^{\beta_2-1} \quad (28)$$

where P_m^{PV} and P_m^{Wind} stand for the rated renewable generation, α_1 , β_1 , α_2 and β_2 are the Beta distribution parameters.

With the objective of minimizing the microgrid operational cost, the scenario-based day-ahead scheduling problem F_d is presented as follows:

$$F_d : \min \frac{1}{S} \sum_{s=1}^S \sum_{t=1}^T \sum_i \left(a^{g,i} (P_{s,t}^{g,i})^2 + b^{g,i} P_{s,t}^{g,i} + c^{g,i} u_t^{g,i} \right) + \sum_{t=1}^T \sum_k \sum_{i \neq j} Z_t^{k,ij} P^{fuel} \quad (29)$$

$$s.t. 0 \leq P_{s,t}^{g,i} \leq u_t^{g,i} P_m^{g,i} \quad (30)$$

where S is the scenario number, $a^{g,i}$, $b^{g,i}$, and $c^{g,i}$ are the generation cost parameters of MT i [35], $P_m^{g,i}$ is the rated MT generation power, p^{fuel} is hourly ice transportation cost.

Note that the optimization variables include the fast-response variables and slow-response variables. The fast-response variables would be changed correspondingly according to the renewable generation deviation in scenario s , which include $H_{s,t}^{ice,k,i}$, $E_{s,t}^{ice,k}$, $P_{s,t}^{icemaking,i}$, $P_{s,t}^{melt,i}$, $E_{s,t}^{AC,i}$, $P_{s,t}^{chiller,i}$, $H_{s,t}^{l,i}$, $P_{s,t}^i$, $P_{s,t}^{g,i}$, $Q_{s,t}^i$, $Q_{s,t}^{g,i}$, $P_{s,t}^{ij}$, $Q_{s,t}^{ij}$, $\ell_{s,t}^{ij}$ and $v_{s,t}^i$. The slow-response variable would remain the same regard to multiple scenarios, which include $Z_t^{k,ij}$ and unit start-stop sign $u_t^{g,i}$. By solving the day-ahead scheduling model, the slow-regulation variable decisions would be obtained and passed on to the real-time stage.

B. REAL-TIME SCHEDULING STAGE

In the real-time stage, model predictive control (MPC) method is used to optimize the microgrid operational cost according to the actual renewable generation power. The scheduling problem F_r is presented as follows:

$$F_r : \min \sum_{\tau=t}^{t+M-1} \sum_i \left(a^{g,i} (P_{\tau}^{g,i})^2 + b^{g,i} P_{\tau}^{g,i} + c^{g,i} u_{\tau}^{g,i} \right) + \sum_{\tau=t}^{t+M-1} \sum_k \sum_{i \neq j} Z_{\tau}^{k,ij} p^{fuel} \quad (31)$$

$$s.t. Z_{\tau}^{k,ij} = \hat{Z}_{\tau}^{k,ij} \quad (32)$$

$$u_t^{g,i} = \hat{u}_t^{g,i} \quad (33)$$

where M is the forecasting time window, $\hat{Z}_{\tau}^{k,ij}$ and $\hat{u}_t^{g,i}$ are the day-ahead decisions.

However, the two-stage scheduling model includes many binary variables and nonlinear constraints, which makes it difficult to be solved. This problem would be addressed in Section V.

V. SOLUTION ALGORITHM

In this section, linearization techniques and Lagrange solution method are used to solve the MG scheduling problem.

A. LINEARIZATION STAGE

The nonlinear constraint (24) makes the scheduling model difficult to be solved. According to [33], (24) is treated as follows:

$$\ell_t^{ij} v_t^i \geq (P_t^{ij})^2 + (Q_t^{ij})^2 \quad (34)$$

$$\left\| \begin{matrix} 2P_t^{ij} \\ 2Q_t^{ij} \\ \ell_t^{ij} - v_t^i \end{matrix} \right\|_2 \leq \ell_t^{ij} + v_t^i \quad (35)$$

Through the above process, the optimization problem is converted as a classic mixed-integer second-order cone programming problem (MISCP).

B. LAGRANGE SOLUTION STAGE

Due to numerous variables and constraints, the MISCP problem is still difficult to be solved. Taking the day-ahead scheduling model as an example, Lagrange solution method is used to solve the optimization problem. The detailed explanations are presented as follows:

By analyzing the day-ahead scheduling model, it can be seen that the optimization problem of the proposed CPCSS includes the ice transportation scheduling (i.e., (1)-(6)) and energy scheduling (i.e., (7)-(26) and (30)). Additionally, the binary variable $Z_t^{k,ii}$ is the only associated variable between them. Therefore, by introducing Lagrange multipliers $\lambda_t^{k,ii}$, the objective function can be relaxed to F_{d-} , as follows:

$$F_{d-} : \min \frac{1}{S} \sum_{s=1}^S \sum_{t=1}^T \sum_i \left(a^{g,i} (P_{s,t}^{g,i})^2 + b^{g,i} P_{s,t}^{g,i} + c^{g,i} u_t^{g,i} \right) + \sum_{t=1}^T \sum_k \sum_{i \neq j} Z_t^{k,ij} p^{fuel} + \sum_{t=1}^T \sum_k \lambda_t^{k,ii} \left(\overline{Z}_t^{k,ii} - Z_t^{k,ii} \right) \quad (36)$$

where $\overline{Z}_t^{k,ii}$ is the decision variable in the energy scheduling problem.

On this basis, two sub-problems are formulated to denote the energy scheduling and ice transportation scheduling, as follows:

Sub-problem 1: energy scheduling

The energy scheduling problem F_{d1-} is formulated as follows:

$$F_{d1-} : \min \frac{1}{S} \sum_{s=1}^S \sum_{t=1}^T \sum_i \left(a^{g,i} (P_{s,t}^{g,i})^2 + b^{g,i} P_{s,t}^{g,i} + c^{g,i} u_t^{g,i} \right) + \sum_{t=1}^T \sum_k \lambda_t^{k,ii} \overline{Z}_t^{k,ii} \quad (37)$$

s.t. (7) – (26), and(30).

Sub-problem 2: ice transportation scheduling

The ice transportation scheduling problem F_{d2-} is formulated as follows:

$$F_{d2-} : \min \sum_{t=1}^T \sum_k \sum_{i \neq j} Z_t^{k,ij} p^{fuel} - \sum_{t=1}^T \sum_k \lambda_t^{k,ii} Z_t^{k,ii} \quad (38)$$

s.t. (1) – (6).

We can see that the sub-problem 1 and sub-problem 2 are linked by Lagrange multipliers $\lambda_t^{k,ii}$. By regulating $\lambda_t^{k,ii}$, an optimal result would be obtained through iterative solu-

tion. In this paper, if $\lambda_t^{k,ii} \neq 1$, it is calculated as follows.

$$\lambda_t^{k,ii,iter+1} = \lambda_t^{k,ii,iter} + \alpha^{iter} (\overline{Z_t^{k,ii}} - Z_t^{k,ii}) \quad (39)$$

where

$$\lambda_t^{k,ii,iter+1} = \lambda_t^{k,ii,iter} + \alpha^{iter} (\overline{Z_t^{k,ii}} - Z_t^{k,ii}) \quad (40)$$

The solution step is expressed as follows:

Step 1: Initialize parameters

Set $\lambda_t^{k,ii,1} = 0$, $F_{d-}^1 = +\infty$, $F_{d-}^1 = -\infty$, and maximum iteration number $Iterm$.

Step 2: Calculate F_{d-}^{iter}

According to $\lambda_t^{k,ii,1,iter}$, update F_{d1-}^{iter} and F_{d2-}^{iter} . On this basis, $F_{d-}^{iter} = \min\{F_{d1-}^{iter}, F_{d2-}^{iter}, F_{d-}^{iter-1}\}$ is calculated.

Step 3: Calculate F_d^{iter}

Following the decision result of $Z_t^{k,ii}$ in Sub-problem 2, calculate the scheduling problem F_d . The result is written as F_d^* . Update $F_d^{iter} = \min\{F_d^{iter-1}, F_d^*\}$.

Step 4: Check stopping criteria

If either $iter > Iterm$ or $F_d^{iter} - F_{d-}^{iter} \leq \varepsilon$ is satisfied, the iteration would be stopped. Or else, let $iter = Iterm + 1$ and go to step 2.

The solution process is depicted in Figure. 3. Note that optimization problem is non-convex and nonlinear, we will use the commercial solver Gurobi to solve it.

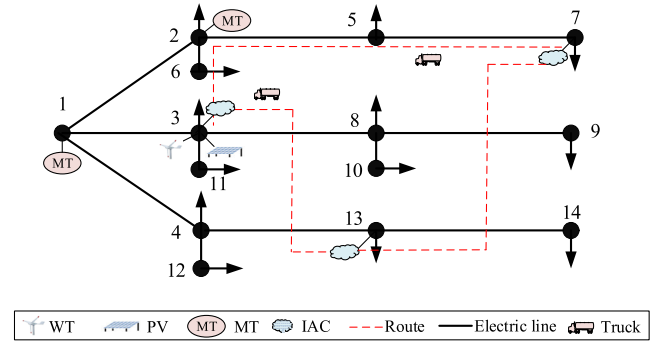


FIGURE 4. Structure of the islanded microgrids with CPCSS.

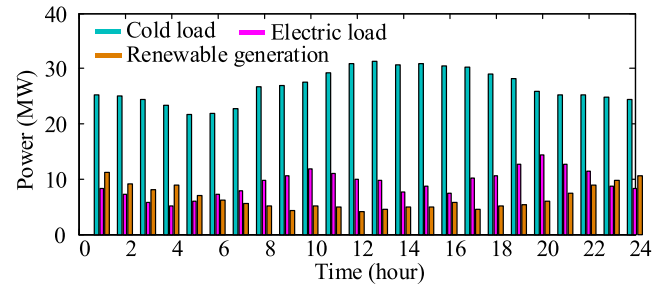


FIGURE 5. Renewable generation and electric and cold load.

TABLE 1. Branch parameters of microgrids.

Branch	R (p.u.)	X (p.u.)	Branch	R (p.u.)	X (p.u.)
1-2	0.15	0.20	1-3	0.22	0.22
1-4	0.22	0.22	2-5	0.18	0.36
2-6	0.16	0.22	5-7	0.08	0.08
3-8	0.16	0.22	8-9	0.16	0.22
8-10	0.22	0.22	3-11	0.22	0.22
4-12	0.18	0.24	4-13	0.08	0.22
13-14	0.08	0.08			

IACs are 5 MW, 2 MW, and 3 MW, respectively. The working efficiencies in three modes are 4.2, 2.8, and 42.5, respectively [29]. The ice retention rate is set to 0.99. The microgrid branch parameters are shown in Tab. 1. Figure 5 shows the wind generation, electric load, and cooling load, where the electric power profiles refer to [37], and the cooling load is collected from tropical regions. On this basis, they a. The microgrid voltages are allowed to operate between 0.93 and 1.07 [38].

According to China’s market prices, the purchase price and service life of trucks are 200000 yuan and 15 years, respectively. Without loss of generality, it is assumed that the ice distribution between IACs can be completed in an hour. The hourly ice distribution cost and daily driver wage are set to 200 yuan and 300 yuan, respectively.

To verify the superiority of the proposed model, three cases are discussed, as follows:

1) Case 1: The cold energy could not be directly exchanged among IACs. The day-ahead dispatching objective is given as follows:

$$F_d : \min \frac{1}{S} \sum_{s=1}^S \sum_{t=1}^T \sum_i \left(a^{g,i} (P_{s,t}^{g,i})^2 + b^{g,i} P_{s,t}^{g,i} + c^{g,i} u_t^{g,i} \right) \quad (41)$$

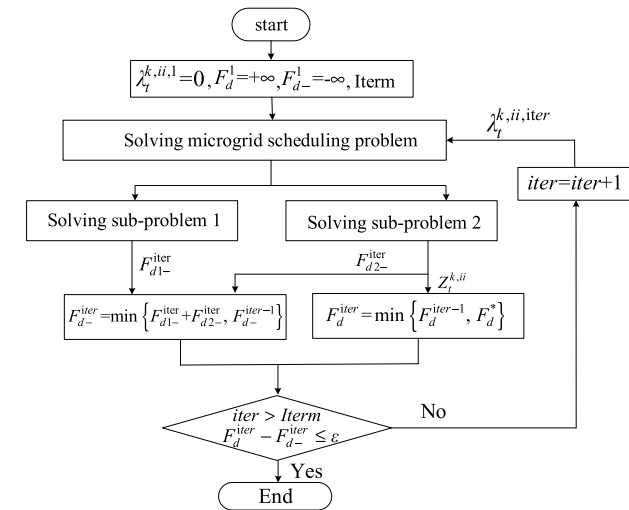


FIGURE 3. Flowchart of the Lagrange solution method.

VI. RESULTS AND DISCUSSION

A. TEST SYSTEM

An IEEE 14-node power grid is used to evaluate the performance of the proposed dispatching strategy [36]. The microgrid structure diagram is shown in Figure 4. As depicted from the figure, three IACs are located at nodes 3, 7, and 13, respectively. The WTs and PVs are installed at nodes 3 and 9. Two MTs are equipped at nodes 1 and 2

The MT generation parameters are $a^{g,i} = 0.001805$ yuan/kw², $b^{g,i} = 0.52575$ yuan/kw, and $c^{g,i} = 9$ yuan [35]. The rated refrigeration power, ice making power, ice-melting power of

2) Case 2: The proposed scheduling model integrating one truck in this paper is used.

3) Case 3: The proposed scheduling model integrating two trucks in this paper is used.

All numerical simulations are coded in MATLAB based on a Windows-based PC with i7 CPU, and 16 GB RAM. The computational time is 147 seconds in case 1, 241 seconds in case 2 and 387 seconds in case 3, respectively.

B. RESULT ANALYSIS

1) ENERGY CONSUMPTION ON THE LONG-TIME SCALE

Figure. 6 shows the CPCSS energy consumption in case 1. As observed from the figure, the MTs and IACs are coordinated to maintain the electric power balance. The MT power varies between 2.4 MW and 18.9 MW, and the corresponding average generation cost floats within 800.9 yuan/MWh and 815.5 yuan/MWh. In the dispatching cycle, the MT generates 264.82 MWh electricity, and the network loss is 5.4 MWh.

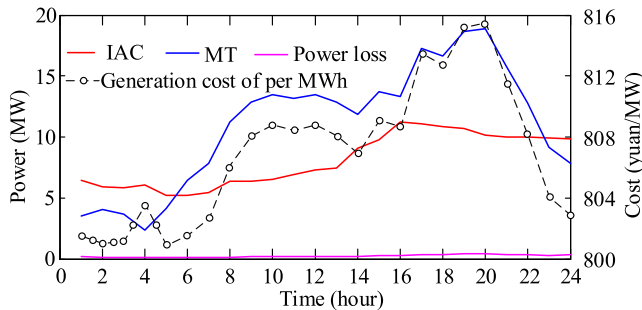


FIGURE 6. CPCSS energy consumption in case 1.

Tab. 2 shows the ice distribution routes in case 2. Assume → stands for the truck driving direction. As observed from the table, the trucks are used to transport ices among IACs. In the dispatching period, ice distribution sequence is 1→2→3→2→1. It can be speculated that the cooling energy exchange in multiple areas are achieved in this case.

TABLE 2. Ice distribution sequences.

Time	1:00-2:00	3:00-4:00	19:00-20:00	22:00-23:00
Trip	1→2	2→3	3→2	2→1

Figure. 7 shows the CPCSS energy consumption based on one truck. Benefiting from the cold energy exchange among multiple areas, the IACs are operated more flexibly, which makes MT work at economical range. In the dispatching cycle, the MT power changes from 1.9 MW to 15.5 MW, and the generation cost fluctuates between 800.9 yuan/MWh and 811.3 yuan/MWh. The MT generation power and network loss are reduced to 245.3 MWh and 4.4 MWh, respectively.

Tab. 3 shows the ice distribution sequences in cases 3. As observed from the table, truck 1 and truck 2 follow trips 1→3→1, and 1→2→1 to transport ices among IACs, respectively. Benefiting from the truck coordination, multiple IACs can exchange cooling energy simultaneously

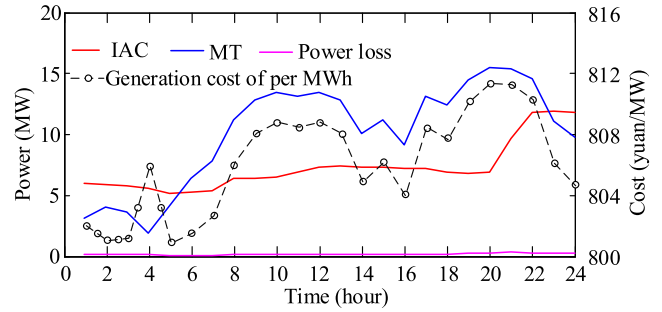


FIGURE 7. CPCSS energy consumption in case 2.

TABLE 3. Ice distribution sequences.

Truck 1	Time	0:00-1:00	22:00-23:00
	Trip	1→3	3→1
Truck 2	Time	1:00-2:00	22:00-23:00
	Trip	1→2	2→1

(e.g. at 22:00-23:00). Therefore, the performance of the cooling and power combined supply would be better.

Figure. 8 verifies the cooling and power combined supply advantages. With the help of two trucks, the energy consumption elasticity of the cooling load is further released. As a result, the MT power could be operated at between 3.1 MW and 14.7 MW. During this range, the average generation cost floats from 800.8 yuan/MWh to 810.3 yuan/MWh. In the dispatching cycle, the MT generation electricity and network loss are further reduced to 231.3 MWh and 3.9 MWh, respectively.

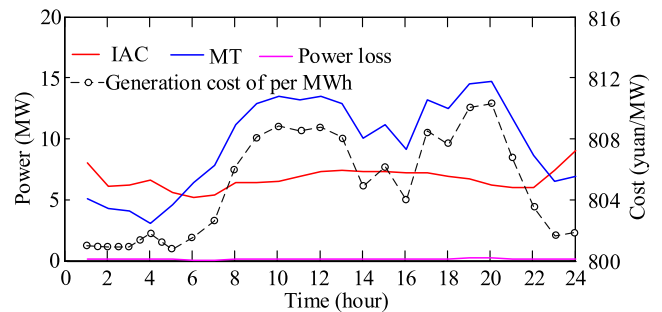


FIGURE 8. CPCSS energy consumption in case 3.

According to the above results, we can see that the MT generation cost and network loss in case 2 and case 3 are smaller than those in case 1, implying the energy saving advantages of the proposed scheduling strategy. Additionally, the result difference in case 2 and 3 indicates that a more closely CPCSS could further improve the microgrid operation performance.

2) POWER SMOOTHING ON THE SHORT-TIME SCALE

Taking the renewable power at 19:00-20:00 in Figure. 9 as an example, the power smoothing performance of the CPCSS on

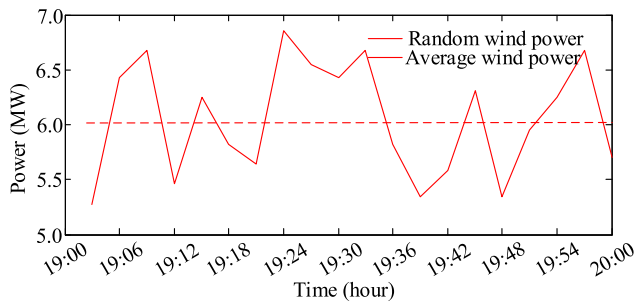


FIGURE 9. Renewable power on the short-time scale.

the short-time scale is introduced. The results are presented as follows:

Figure. 10 depicts the power smoothing effect in case 1. As observed from the figure, the IAC closely follows the renewable generation fluctuation. However, the IAC power variation amplitude is limited to 0.36 MW due to the operational constraint. As a result, the MTs are simultaneously regulated to maintain the power balance, resulting in a floating generation cost. In this hour, the average generation cost (i.e., upper bound of grey zone) is 813.7 yuan per MWh. In contrast, the nominal generation cost without responding to the power fluctuation (i.e., lower bound of grey zone) is only 812.3 yuan per MWh. The results show the renewable generation fluctuation could increase the actual generation cost of MTs.

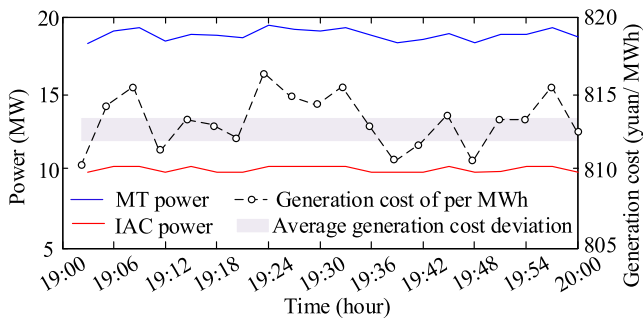


FIGURE 10. Power smoothing on the short-time scale in case 1.

Figure. 11 shows the power smoothing performance in case 2. Unlike in case 1, the IACs could deeply participate in the renewable generation smoothing. Its power variation range is within 6.65 MW-7.25 MW. In this case, the average and nominal generation costs of the MTs are 810.9 and 810.4 yuan per MWh, respectively. The hourly cost deviation of 0.5 yuan per MWh implies that the impact of the power fluctuation is significantly mitigated

Figure. 12 is the operation power on the short-time scale in case 3. The IACs are allowed to work at between 5.85 MW and 6.49 MW. Benefiting from the IAC regulation effect, the MT power variation amplitude is reduced. The average generation cost of the MTs is 808.9 yuan per MWh, which is only 0.4 yuan per MWh higher than the nominal cost.

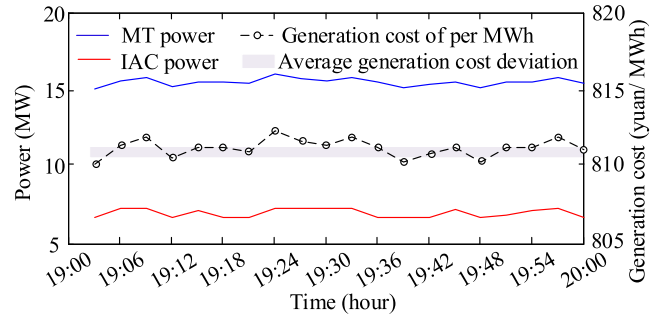


FIGURE 11. Power smoothing on the short-time scale in case 2.

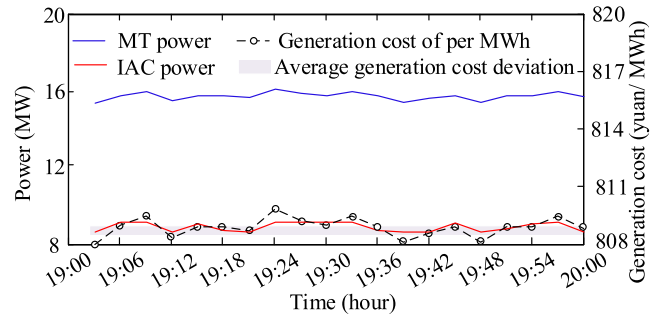


FIGURE 12. Power smoothing on the short-time scale in case 3.

In summary, the proposed scheduling strategy could release the IAC regulation ability on the short-time scale, and reduce the renewable fluctuation impact.

3) ECONOMY ANALYSIS

Table 4 shows the microgrid comprehensive operation costs in three cases. According to the daily cost of the MT and fuel, we can calculate that the microgrid annual operation costs are 78077150 yuan in case 1, 72160500 yuan in case 2, and 67959350 yuan in case 3, respectively.

TABLE 4. MG comprehensive costs.

	MT daily cost (yuan)	Fuel daily cost (yuan)	Driver annual cost (yuan)	Truck annual depreciation cost (yuan)	Total annual cost (yuan)
Case 1	213910	0	0	0	78077150
Case 2	197700	800	109500	15000	72285000
Case 3	186190	800	219000	30000	68208350

According to the domestic market information, the truck sale price is 150000 yuan, respectively. Assume that the truck service life is 10 years, the annual operation costs of the microgrid are 78077150 yuan in case 1, 72285000 yuan in case 2, and 68208350 yuan in case 3, respectively.

Compared that in case 1 and 2, the MG cost in case 3 could be reduced by 9868800 yuan (12.6%) and 4076650 yuan (5.6%), respectively. The result shows that the proposed scheduling strategy could significantly improve the microgrid operation economy.

C. IMPACT OFFUEL PRICES

To increase the persuasion, the impact of the fuel price is studied. Assume the fuel price in the original manuscript as

1.0, Fig. 13 depicts the microgrid operation cost in three cases with a price of 0.7~1.3.

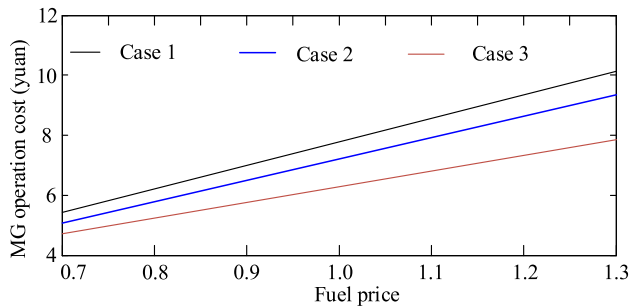


FIGURE 13. Impact of fuel prices on the MG operational costs.

As observed from the figure, With the increase of the fuel price, the MG operation costs in three cases increase simultaneously. However, the MG operation costs in case 1, 2, and 3 are always highest, moderate, and lowest, respectively. Additionally, as the fuel price increases from 0.7 to 1.3, compared with that in case 1 and case 2, the MG operation cost in case 3 could be reduced by from 6429000 yuan to 12327000 yuan, from 3266600 yuan to 6226800 yuan, respectively. The result shows that the advantages of the proposed scheduling strategy would be more prominent as the fuel price increases.

D. COMPARISON WITH ONE-STAGE SCHEDULING STRATEGY

To verify the superiority of the proposed two-stage scheduling strategy, a one-stage scheduling method integrating MPC is used to guide the microgrid operation [39]. The results are depicted in Table 5.

TABLE 5. MG comprehensive costs.

	MT daily cost (yuan)	Fuel daily cost (yuan)	Driver annual cost (yuan)	Truck annual depreciation cost (yuan)	Total annual cost (yuan)
Case 1	228740	0	0	0	83490100
Case 2	205990	400	109500	15000	75456850
Case 3	194320	400	219000	30000	71321800

As observed from the figure, the annual MG operational costs in three cases are 83490100 yuan, 75456850 yuan, and 71321800 yuan, respectively. Unlike this one-stage dispatching results, the annual MG operational costs using the two-stage strategy could be reduced by 5412950 yuan (6.5%) in case 1, 3171850 yuan (4.2%) in case 2, and 3113450 yuan (4.4%) in case 3, respectively. The results indicate that the proposed scheduling strategy could significantly reduce the MG operation cost.

VII. CONCLUSION

In this paper, a novel cooling and power combined supply scheme is designed. Based on the theory analysis and simulation result, the conclusions could be obtained as follows:

- 1) The proposed integrated cooling and power system could significantly reduce the MG operation cost by shifting consumption shifting and smoothing power simultaneously.
- 2) The proposed two-stage MG scheduling strategy could ensure the CPCSS performance on the multi-time scales.
- 3) The linearized techniques and Lagrange solution method could efficiently solve the scheduling problem.

In the actual scenario, the PDF of uncertainties could not be obtained. Therefore, future work will include dealing with the severe uncertainties.

REFERENCES

- [1] M. Tavakoli, F. Shokridehaki, M. Marzband, R. Godina, and E. Pournesmaeil, "A two stage hierarchical control approach for the optimal energy management in commercial building microgrids based on local wind power and PEVs," *Sustain. Cities Soc.*, vol. 41, pp. 332–340, Aug. 2018.
- [2] Q. Sui, F. Wei, R. Zhang, X. Lin, N. Tong, Z. Wang, and Z. Li, "Optimal use of electric energy oriented water-electricity combined supply system for the building-integrated-photovoltaics community," *Appl. Energy*, vol. 247, pp. 549–558, Aug. 2019.
- [3] C. D. Korkas, S. Baldi, I. Michailidis, and E. B. Kosmatopoulos, "Occupancy-based demand response and thermal comfort optimization in microgrids with renewable energy sources and energy storage," *Appl. Energy*, vol. 163, pp. 93–104, Feb. 2016.
- [4] M. Tavakoli, F. Shokridehaki, M. F. Akorede, M. Marzband, I. Vechiu, and E. Pournesmaeil, "CVaR-based energy management scheme for optimal resilience and operational cost in commercial building microgrids," *Int. J. Electr. Power Energy Syst.*, vol. 100, pp. 1–9, Sep. 2018.
- [5] G. Pan, W. Gu, Y. Lu, H. Qiu, S. Lu, and S. Yao, "Accurate modeling of a profit-driven power to hydrogen and methane plant toward strategic bidding within multi-type markets," *IEEE Trans. Smart Grid*, vol. 12, no. 1, pp. 338–349, Jan. 2021.
- [6] J. Hao, Q. Chen, K. He, L. Chen, Y. Dai, F. Xu, and Y. Min, "A heat current model for heat transfer/storage systems and its application in integrated analysis and optimization with power systems," *IEEE Trans. Sustain. Energy*, vol. 11, no. 1, pp. 175–184, Jan. 2020.
- [7] Y. Jiang, C. Wan, A. Botterud, Y. Song, and S. Xia, "Exploiting flexibility of district heating networks in combined heat and power dispatch," *IEEE Trans. Sustain. Energy*, vol. 11, no. 4, pp. 2174–2188, Oct. 2020.
- [8] C. Lin, W. Wu, B. Wang, M. Shahidehpour, and B. Zhang, "Joint commitment of generation units and heat exchange stations for combined heat and power systems," *IEEE Trans. Sustain. Energy*, vol. 11, no. 3, pp. 1118–1127, Jul. 2020.
- [9] S. Yao, W. Gu, S. Lu, S. Zhou, Z. Wu, G. Pan, and D. He, "Dynamic optimal energy flow in the heat and electricity integrated energy system," *IEEE Trans. Sustain. Energy*, vol. 12, no. 1, pp. 179–190, Jan. 2021.
- [10] J. Yang, A. Botterud, N. Zhang, Y. Lu, and C. Kang, "A cost-sharing approach for decentralized Electricity–Heat operation with renewables," *IEEE Trans. Sustain. Energy*, vol. 11, no. 3, pp. 1838–1847, Jul. 2020.
- [11] Z. Li, W. Wu, M. Shahidehpour, J. Wang, and B. Zhang, "Combined heat and power dispatch considering pipeline energy storage of district heating network," *IEEE Trans. Sustain. Energy*, vol. 7, no. 1, pp. 12–22, Jan. 2016.
- [12] Z. Li, W. Wu, J. Wang, B. Zhang, and T. Zheng, "Transmission-constrained unit commitment considering combined electricity and district heating networks," *IEEE Trans. Sustain. Energy*, vol. 7, no. 2, pp. 480–492, Apr. 2016.
- [13] Y. Cao, W. Wei, L. Wu, S. Mei, M. Shahidehpour, and Z. Li, "Decentralized operation of interdependent power distribution network and district heating network: A market-driven approach," *IEEE Trans. Smart Grid*, vol. 10, no. 5, pp. 5374–5385, Sep. 2019.
- [14] S. Lu, W. Gu, S. Zhou, W. Yu, S. Yao, and G. Pan, "High-resolution modeling and decentralized dispatch of heat and electricity integrated energy system," *IEEE Trans. Sustain. Energy*, vol. 11, no. 3, pp. 1451–1463, Jul. 2020.
- [15] H. Zhou, Z. Li, J. H. Zheng, Q. H. Wu, and H. Zhang, "Robust scheduling of integrated electricity and heating system hedging heating network uncertainties," *IEEE Trans. Smart Grid*, vol. 11, no. 2, pp. 1543–1555, Mar. 2020.

- [16] N. Neyestani, M. Yazdani-Damavandi, M. Shafie-khah, G. Chicco, and J. P. S. Catalao, "Stochastic modeling of multienergy carriers dependencies in smart local networks with distributed energy resources," *IEEE Trans. Smart Grid*, vol. 6, no. 4, pp. 1748–1762, Jul. 2015.
- [17] R. Z. Wang, X. Yu, T. S. Ge, and T. X. Li, "The present and future of residential refrigeration, power generation and energy storage," *Appl. Thermal Eng.*, vol. 53, no. 2, pp. 256–270, May 2013.
- [18] G. Salvalai, J. Pfaffert, and M. M. Sesana, "Assessing energy and thermal comfort of different low-energy cooling concepts for non-residential buildings," *Energy Convers. Manage.*, vol. 76, pp. 332–341, Dec. 2013.
- [19] Z. Wang, S. Sun, X. Lin, C. Liu, N. Tong, Q. Sui, and Z. Li, "A remote integrated energy system based on cogeneration of a concentrating solar power plant and buildings with phase change materials," *Energy Convers. Manage.*, vol. 187, pp. 472–485, May 2019.
- [20] F. Wei, Y. Li, Q. Sui, X. Lin, L. Chen, Z. Chen, and Z. Li, "A novel thermal energy storage system in smart building based on phase change material," *IEEE Trans. Smart Grid*, vol. 10, no. 3, pp. 2846–2857, May 2019.
- [21] G. E. D. Plessis, L. Liebenberg, and E. H. Mathews, "The use of variable speed drives for cost-effective energy savings in south African mine cooling systems," *Appl. Energy*, vol. 111, pp. 16–27, Nov. 2013.
- [22] P. Maré, J. H. Marais, and J. V. Rensburg, "Improved implementation strategies to sustain energy saving measures on mine cooling systems," in *Proc. Int. Conf. Ind. Commercial Energy (ICUE)*, Aug. 2015, pp. 102–109.
- [23] Y. Fu, W. Zuo, M. Wetter, J. W. VanGilder, and P. Yang, "Equation-based object-oriented modeling and simulation of data center cooling systems," *Energy Buildings*, vol. 198, pp. 503–519, Sep. 2019.
- [24] M. Iyengar and R. Schmidt, "Analytical modeling for thermodynamic characterization of data center cooling systems," *J. Electron. Packag.*, vol. 131, no. 2, pp. 51–59, Jun. 2009.
- [25] M. Lionello, R. Lucchese, M. Rampazzo, M. Guay, and K. Atta, "Energy-efficient operation of indirect adiabatic data center cooling systems via Newton-like phasor extremum seeking control," *Int. J. Adapt. Control Signal Process.*, pp. 1–18, 2021, doi: 10.1002/acs.3223.
- [26] E. Pakbaznia and M. Pedram, "Minimizing data center cooling and server power costs," in *Proc. 14th ACM/IEEE Int. Symp. Low power Electron. design (ISLPED)*, San Francisco, CA, USA, Aug. 2009, pp. 145–150.
- [27] T. Jiang, P. Ju, C. Wang, H. Li, and J. Liu, "Coordinated control of air-conditioning loads for system frequency regulation," *IEEE Trans. Smart Grid*, vol. 12, no. 1, pp. 548–560, Jan. 2021.
- [28] N. Mahdavi, J. H. Braslavsky, and C. Perfumo, "Mapping the effect of ambient temperature on the power demand of populations of air conditioners," *IEEE Trans. Smart Grid*, vol. 9, no. 3, pp. 1540–1550, May 2018.
- [29] J.-A. Huang, T.-T. Ha, and Y.-J. Zhang, "An optimal control method of ice-storage air conditioning based on reducing direct cooling cost sequentially," in *Proc. IEEE Int. Conf. Power Renew. Energy (ICPRE)* Oct. 2016, pp. 264–268.
- [30] C.-C. Lo, S.-H. Tsai, and B.-S. Lin, "Ice storage air-conditioning system simulation with dynamic electricity pricing: A demand response study," *Energies*, vol. 9, no. 2, pp. 20–113, 2016.
- [31] W.-S. Lee, Y.-T. Chen, and T.-H. Wu, "Optimization for ice-storage air-conditioning system using particle swarm algorithm," *Appl. Energy*, vol. 86, no. 9, pp. 1589–1595, Sep. 2009.
- [32] *Ice Transport for Relieving Summer Heat*. Accessed: Nov. 21, 2020. [Online]. Available: <https://news.eastday.com/s/20160630/u1ai9488831.html>
- [33] G. Pan, W. Gu, Y. Lu, H. Qiu, S. Lu, and S. Yao, "Optimal planning for electricity-hydrogen integrated energy system considering power to hydrogen and heat and seasonal storage," *IEEE Trans. Sustain. Energy*, vol. 11, no. 4, pp. 2662–2676, Oct. 2020.
- [34] Q. Sui, R. Zhang, C. Wu, F. Wei, X. Lin, and Z. Li, "Stochastic scheduling of an electric vessel-based energy management system in pelagic clustering islands," *Appl. Energy*, vol. 259, Feb. 2020, Art. no. 114155.
- [35] A. Maulik and D. Das, "Optimal operation of a droop-controlled DCMG with generation and load uncertainties," *IET Gener., Transmiss. Distrib.*, vol. 12, no. 12, pp. 2905–2917, Jul. 2018.
- [36] *IEEE 14 Node Distribution Network*. Accessed: Nov. 21, 2020. [Online]. Available: <https://wenku.baidu.com/view/a5eda49a51e79b896802269b?pcf=2&bfetype=new>
- [37] M. Xue, B. Zhao, X. Zhang, and Q. Jiang, "Integrated plan and evaluation of grid-connected microgrid," *Automat. Electr. Power Syst.*, vol. 39, no. 3, pp. 6–13, Feb. 2015.
- [38] Q. Sui, F. Wei, X. Lin, C. Wu, Z. Wang, and Z. Li, "Multi-energy-storage energy management with the robust method for distribution networks," *Int. J. Electr. Power Energy Syst.*, vol. 118, Jun. 2020, Art. no. 105779.
- [39] M. Song, C. Gao, H. Yan, and J. Yang, "Thermal battery modeling of inverter air conditioning for demand response," *IEEE Trans. Smart Grid*, vol. 9, no. 6, pp. 5522–5534, Nov. 2018.



JUNYU LIANG was born in Yunnan, China, in 1983. He received the M.D. degree from North China Electric Power University, in 2012.

He is currently an Engineer with the Electric Power Research Institute, Yunnan Power Grid Company Ltd. His research interests include wind power generation and integrated energy services.



ZHAO LUO (Member, IEEE) received the B.S. degree in electronic science and technology from the Nanjing University of Posts and Telecommunications, China, in 2008, and the M.S. and Ph.D. degrees in electrical engineering from Southeast University, China, in 2013 and 2018, respectively.

He is currently an Associate Professor with the Faculty of Electric Power Engineering, Kunming University of Science and Technology. His research interests include distributed generations and microgrids, and active distribution networks.



XINGYU YUAN is currently an Engineer with the Electric Power Research Institute, Yunnan Power Grid Company Ltd. His research interests include renewable energy technology and active distribution networks.

JIALU GENG is currently pursuing the master's degree with the Faculty of Electric Power Engineering, Kunming University of Science and Technology, Kunming, China. His research interests include distributed generations and microgrids.

HONGZHI LIU is currently pursuing the master's degree with the Faculty of Electric Power Engineering, Kunming University of Science and Technology, Kunming, China. His research interests include distributed generations and microgrids.

JIAQUAN YANG is currently with the Electric Power Research Institute, Yunnan Power Grid Company Ltd. His research interests include active distribution networks and power system operation.

MIN DONG is currently pursuing the master's degree with the Faculty of Electric Power Engineering, Kunming University of Science and Technology, Kunming, China. His research interests include distributed generations and microgrids.

YINGHAO DAI is currently pursuing the master's degree with the Faculty of Electric Power Engineering, Kunming University of Science and Technology, Kunming, China. His research interests include distributed generations and microgrids.

...